METHODOLOGY

Novel hybrid SCA-XGB model for compressive strength of concrete at elevated temperatures

Thi-Quynh Nguyen[1] · Trong-Cuong Vo[1] · Thi-Thu Hien Nguyen[1] · Viet-Linh Tran[1]

Abstract

Compressive strength is a primary factor of concrete. Concrete characteristic severely affects by temperatures, which can reduce the strength properties of the concrete. Therefore, the accurate prediction of the concrete compressive strength at elevated temperatures is challenging. This study aims to develop a robust hybrid SCA-XGB model that integrated a sine cosine algorithm and an extreme gradient boosting model, to precisely predict the compressive strength of concrete at elevated temperatures. First, the database of concrete strength at different temperatures is collected from the literature. Then, hybrid SCA-XGB models are developed with the assistance of the SCA algorithm for fining-tune the hyperparameters of the XGB model for predicting the compressive strength at elevated temperatures. As a result, several hybrid SCA-XGB models are generated by changing the training-test ratio of database and the population size of the SCA algorithm. The best hybrid SCA-XGB model is chosen by evaluating the statistical metrics. The performance of the best SCA -XGB model is compared with those of other machine learning (ML) models. The SCA-XGB model achieves credible results with (0.995, 0.982) of R^2, (0.925 and 0.810) of A10, (1.774 MPa and 3.676 MPa) of RMSE, and (1.317 MPa and 2.706 MPa) of MAE. It is found that the SCA-XGB model not only accurately predicts the compressive strength of concrete at elevated temperatures but also outperforms other models. Notably, the black box behind the SCA-XGB model is explored using the SHapley Additive exPlanation (SHAP) method via the global and local explanations. Finally, a web application is built based on the SCA-XGB model for users can rapidly predict the compressive strength of concrete at elevated temperatures.

Keywords Concrete strength · Elevated temperatures · Extreme gradient boosting · Sine cosine algorithm · Web application

Introduction

Concrete is a commonly used material in engineering structures. The advantages of concrete include but are not limited to durability, porosity, acoustic insulation, impact resistance, and fire resistance (Dong et al., 2019). Therefore, it can be used for buildings, tunnels, reservoirs, dams, or bridges (Chica & Alzate, 2019). As urbanization progresses, concrete has become an increasingly important material (Reiter et al., 2020).

Generally, structures are prone to be subjected to fire or high temperatures during their life due to many effects (Roy & Matsagar, 2021). Although in terms of fire resistance and heat resistance, concrete is considered one of the best materials (Ma et al., 2015), high temperature not only severely affects the physical, chemical, and mechanical properties of concrete (An et al., 2020; Gupta et al., 2020; Nguyen et al., 2020) but also makes the concrete reduce its mechanical properties, resulting in the loss of its durability (Karahan, 2017), and causing the spalling of concrete (Li et al., 2021). Therefore, it is hard to accurately estimate the concrete strength at elevated temperatures because of highly complex properties and temperature-dependent parameters.

The performance behaviors of ordinary, high-performance, and lightweight concrete at high temperatures were experimentally investigated in previous studies (Chan et al., 2000; Husem, 2006; Kim et al., 2002; Masaki & Maki, 2002; Memon et al., 2019; Tanyildizi & Coskun, 2008). It was found that casting and curing to estimate concrete behaviors at high temperatures are considered a challenging task. Recent years have seen a considerable increase in the use of machine learning (ML) to solve complex and nonlinear problems (Salehi & Burgueño, 2018; Thai, 2022). ML

✉ Viet-Linh Tran
  vietlinh.dhv@gmail.com

[1] Department of Civil Engineering, Vinh University,
  Vinh 461010, Vietnam

algorithms are typically applied in civil engineering to predict the mechanical properties of concrete (Dinesh et al., 2023). Although several studies have utilized ML techniques for predicting compressive concrete strength, they are applied to concrete at room temperature (Kaloop et al., 2020; Kaveh & Iranmanesh, 1998; Naderpour et al., 2018; Nguyen et al., 2022a). The application of ML to concrete strength at elevated temperatures is relatively rare. Mukherjee and Nag Biswas (1997) and Abbas et al. (2019) collected a database of concrete under three load conditions to develop an ANN model for predicting the residual strength of high-strength concrete at high temperatures. Ahmad et al. (2021) used an artificial neural network (ANN), decision tree (DT), gradient boosting (GB), and bagging models to predict concrete strength at high temperatures. Although the bagging model outperformed other models, the correlation between prediction and real values is not high ($R^2 = 0.90$).

In various fields of science and engineering, the extreme gradient boosting (XGB) algorithm has proved its potential to address multiple challenges (Huber et al., 2022; Kaveh et al., 2021; Mai et al., 2023; Nguyen et al., 2022b; Tran & Kim, 2023; Tran et al., 2023; Van Nguyen et al., 2022a, 2022b, 2022c). According to the literature, the performance of the XGB model shows more accurate predictions when compared to other ML models. Mirjalili and Gandomi (2023) and Kaveh (2021) proposed several potential metaheuristic optimization algorithms. These algorithms have drawn significant attention from researchers in different fields. Admittedly, each algorithm has its advantages and limitations. In addition, the performance of optimization algorithms depends strongly on the problem solved. In this study, many metaheuristic optimization algorithms have been tested, and the author found that the SCA coupled with XGB, which was not used previously, achieves the best results for predicting compressive concrete strength at elevated temperatures.

In light of this gap, this study aims to predict compressive concrete strength at elevated temperatures using a hybrid SCA-XGB model. The hybridization of SCA with the XGB model can enhance prediction accuracy. The performance of the developed SCA -XGB model is compared with those of other machine learning (ML) models, such as default XGB,

DT, random forest (RF), adaptive gradient boosting (AGB), and GB models. In addition, the black box behind the SCA-XGB model is explored using the SHapley Additive exPlanation (SHAP) method via the global and local explanations. Finally, a web application is built based on the SCA-XGB model for users can rapidly predict the compressive strength of concrete at elevated temperatures.

Database description

This study collects the tests on concrete strength at elevated temperatures from the previous study (Ahmad et al., 2021) to develop hybrid SCA-XGB models. Nine features of concrete that affected the concrete strength (f_c') at elevated temperatures are considered, such as cement (C), water (W), fine aggregate (FA), coarse aggregate (CA), fly ash (FLA), superplasticizer (S), silica fume (SF), nano silica (NS), and temperature (T).

The statistical properties of the database are presented in Table 1. Figure 1 depicts the Pearson correlation coefficient matrix, which reveals the degree of linear relationship between variables in the database. It can be found that temperature has a strong negative correlation with compressive strength at elevated temperatures, indicated by the coefficients of -0.59. C, W, FA, FLA, and S are moderately correlated with compressive strength, indicated by the coefficients of 0.28, -0.31, 0.32, 0.24, and 0.28, respectively. Meanwhile, CA, SF, and NS have a low correlation with compressive strength, indicated by the coefficients of -0.01, -0.13, and 0.14, respectively.

Machine learning and optimization algorithms

Extreme gradient boosting (XGB)

The XGB is an improvement of the gradient boosting (GB) algorithm (Chen & Guestrin, 2016). The XGB utilizes parallel process computing to enhance the training process speed and balance between bias and variance, thereby reducing

Table 1 Statistical properties of the database

	C (kg/m³)	W (kg/m³)	FA (kg/m³)	CA (kg/m³)	FLA (kg/m³)	S (kg/m³)	SF (kg/m³)	NS (kg/m³)	T (kg/m³)	f_c' (MPa)
Min	250.000	123.000	0.000	0.000	0.000	0.000	0.000	0.000	20.000	3.000
Mean	437.686	182.922	610.130	1052.126	12.652	8.581	29.317	1.739	354.522	49.311
Max	786.000	385.000	1345.000	1681.000	150.000	25.900	150.000	22.500	1000.000	133.600
Std	95.491	59.905	317.391	309.412	33.072	7.597	37.086	5.248	287.651	25.170
Cov	0.218	0.327	0.520	0.294	2.614	0.885	1.265	3.018	0.811	0.510

Fig. 1 Pearson correlation coefficient of variables

overfitting. In the XGB, the process involves iteratively training DTs using residuals from previous trees. Accordingly, each DT is built sequentially during training, and each subsequent tree tries to correct previous errors. Figure 2 reveals the flowchart of the XGB algorithm.

Sine cosine algorithm (SCA)

The SCA (Seyedali Mirjalili, 2016) method is based on a population-based probabilistic search. It uses sine and cosine trigonometric functions to update search agents' positions in the population. It is inspired by the periodic nature in the range [−1, 1] of sine and cosine functions, providing great potential for exploring and exploiting the search space.

Similar to any other meta-heuristic algorithm, the SCA initiates randomly representative search agents or solutions in the search space. The search agents in the population can be viewed as vectors in a d-dimensional space. A stochastic equation containing trigonometric sine and cosine functions is used by search agents to update their positions. The ith search agent $X_i = (X_{i1}, X_{i2}, \ldots, X_{id})$ is initialized using the following equation:

$$X_{ij} = X_{ij}^{lb} + rand() \times \left(X_{ij}^{ub} - X_{ij}^{lb} \right), j = 1 : d, i = 1 : N_p, \tag{1}$$

where X_{ij} is the jth dimension of the ith solution, X_{ij}^{lb} and X_{ij}^{ub} are the lower bound and upper bound of the ith solution in the jth dimension, respectively. rand() is a uniformly distributed random number in the range [0, 1], and N_p is the number of search agents (the population size).

The following equations are position update equations of each search agent:

$$X_{ij}^{t+1} = X_{ij}^t + r1 \times \sin(r2) \times \left| r3 \times P_g^t - X_{ij}^t \right|, \tag{2}$$

$$X_{ij}^{t+1} = X_{ij}^t + r1 \times \cos(r2) \times \left| r3 \times P_g^t - X_{ij}^t \right|, \tag{3}$$

where, $X_i^t = (X_{i1}^t, X_{i2}^t, \ldots, X_{id}^t)$ are the position of the ith search agent in the tth iteration. $P_g^t = (P_{g1}^t, P_{g2}^t, \ldots, P_{gd}^t)$ is the gth search agent having the best fitness and considered as the destination point at tth iteration. |.| represents the modulus operator.

$$r1 = b - b \times \left(\frac{t}{T}\right), \tag{4}$$

$$r2 = 2 \times \pi \times rand(), \tag{5}$$

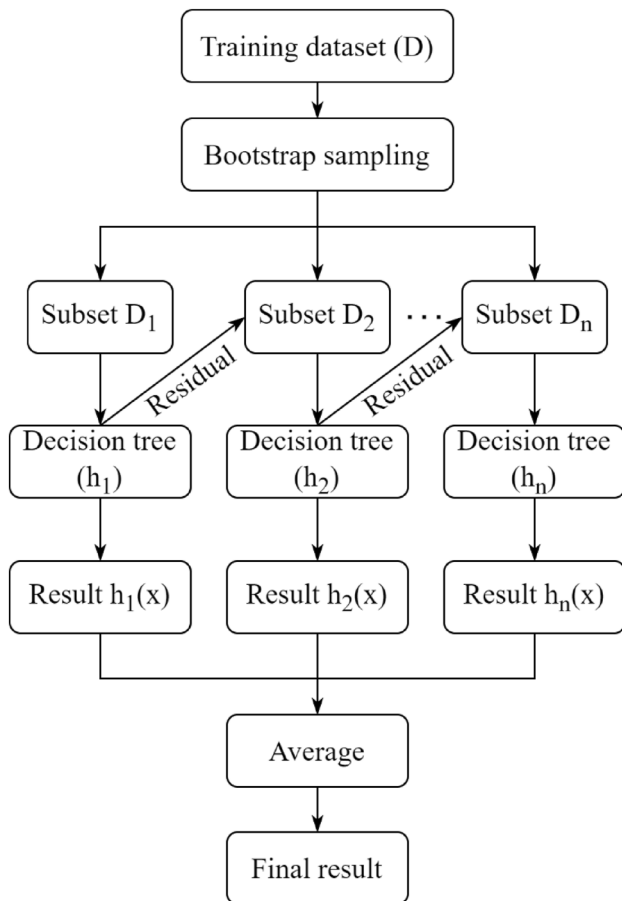$$r3 = 2 \times rand(), \tag{6}$$

Fig. 2 Flowchart of XGB

where b is a constant parameter and T denotes the maximum number of iterations.

r1 controls the movement of X_i, if $r1 < 1$, then X_i moves toward destination point P_g (exploitation step), and when $r1 \geq 1$, the search agent moves far away from the destination point P_g (exploration step). A switch probability p (p = 0.5) is used to determine whether Eqs. (2) or (3) should be used to update the position of the search agents. The p depends on a generated random number $r4 \in [0, 1]$. If $r4 < p$, Eq. (2) is used to update the position of the search agents, otherwise Eq. (3) is used. The flowchart for the SCA is shown in Fig. 3.

Development of hybrid SCA-XGB model

The main steps of developing the SCA-XGB model can be summarized in Fig. 4. To establish SCA-XGB models for predicting concrete strength at elevated temperatures, cement, water, fine aggregate, coarse aggregate, fly ash, superplasticizer, silica fume, nano silica, and temperature are utilized as input variables. The concrete strength is considered an output parameter.

The database is randomly divided into training and test sets, with eight training-to-test set ratios (0.55–0.45, 0.60–0.40, 0.65–0.35, 0.70–0.30, 0.75–0.25, 0.80–0.20, 0.85–0.15, and 0.90–0.10). In addition, different population sizes of SCA ranging from 50 to 300 with increments of 50 are tested. In the ML realm, hyperparameters play a significant role in model performance. Therefore, hyperparameter tuning is critical in developing an ML model. In this study, hyperparameter optimization of the XGB model is done using the SCA. Five-fold cross-validation is utilized during hyperparameter tuning to achieve more reliability and generalization of model performance. Once the optimal hyperparameters are determined based on the training set. The final model is evaluated using the test set. The effectiveness of the XGB model is quantified using various evaluation metrics. This study uses four statistical metrics to assess the model's performance: R^2, A10, RMSE, and MAE. The equations of these metrics can be found in the previous studies (Mai et al., 2023; Nguyen et al., 2022a, 2022b, 2022c; Tran & Kim, 2023). Finally, the XGB model can be deployed as a web application to predict new and unseen data.

The detailed performance of several SCA-XGB models is presented in the Supplemental material. It is generally true that all models perform better during training than during testing. However, the performance of models in the test phase is used to choose the best model on unseen data. Therefore, the population sizes and training-test ratios are considered to establish SCA-XGB models, which are scored from 1 to 48. It is worth noting that a high R^2 and A10 score correlate to a high score, whereas a high RMSE and MAE score correlate to a low score. Accordingly, ML models are scored based on the sum of all evaluation metrics. The best results of the SCA-XGB model are highlighted in bold in the tables in the Supplementary materials. The optimized hyperparameter values of the XGB model are shown in Table 2. The performance of the best SCA-XGB model is presented in Table 3. It can be seen that there is a minor difference between training and test sets, so there is little overfitting in the chosen SCA-XGB model.

Results and discussion

In this study, five other ML models, including DT, random forest (RF), adaptive gradient boosting (AGB), GB, and XGB, are selected to compare their superiority and reliability with the developed SCA-XGB model in predicting the concrete strength at elevated temperatures.

The performance of these models is presented in Table 4. It is evident from the results that the SCA-XGB outperforms the other models, as indicated by its higher R^2 (0.982) and A10 (0.810) values and lower RMSE (3.676 MPa) and MAE (2.706 MPa) values in the test phase, which are bold

Fig. 3 Flowchart of SCA
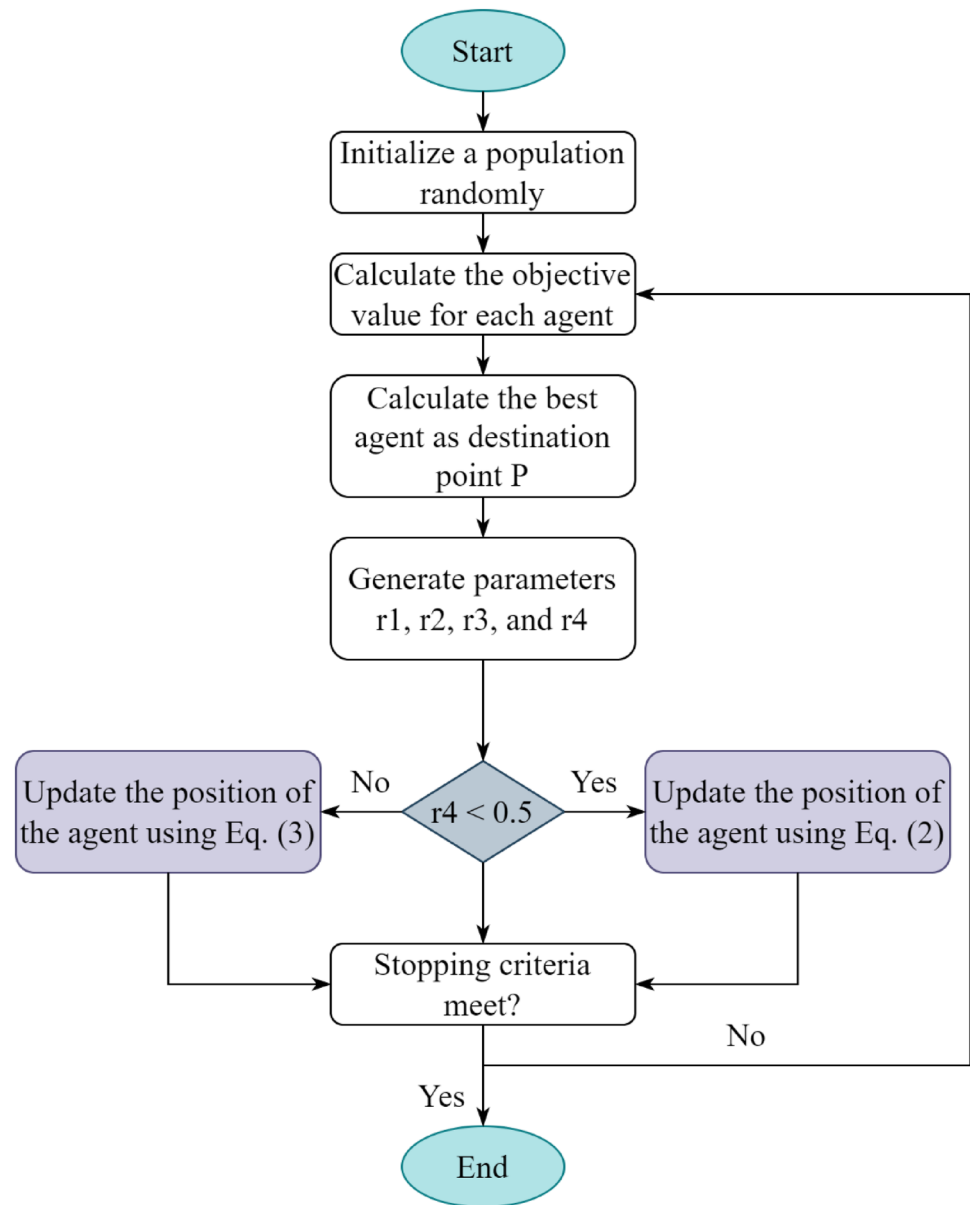
in Table 4. Followed by the XGB model with R^2 of 0.965, A10 of 810, RMSE of 4.604 MPa, and MAE of 3.595 MPa in the test phase. Conversely, the AGB model exhibits the poorest performance with R^2 of 0.927, A10 of 0.381, RMSE of 8.679 MPa, and MAE of 6.735 MPa in the test phase. Compared with the XGB, DT, RF, AGB, and GB models, R^2 and A10 increased by (1.762%, 4.357%, 1.133%, 5.933%, and 1.551%) and (0.0%, 30.856%, 13.445%, 112.598%, and 21.439%), RMSE and MAE decreased by (20.156%, 42.589%, 16.927%, 57.645%, and 24.393%) and (24.729%, 42.911%, 21.406%, 59.822%, and 25.104%), respectively, in the SCA-XGB model in the test phase.

Figure 5 depicts the scatter plot of their predicted and actual concrete strength values. As shown in the figure, the black line represents the ideal scenario where predictions are perfect matches with targets. Based on the figure, it is obvious that the SCA-XGB model is significantly more accurate than other models. In conclusion, the hybrid SCA-XGB model demonstrates greater accuracy and robustness in predicting concrete strength at elevated temperatures. It is found that the SCA proves to be effective in improving the XGB's predictive capability for the given dataset. The hybrid approach exhibits the best performance, leveraging the strengths of both SCA and XGB to achieve superior prediction.
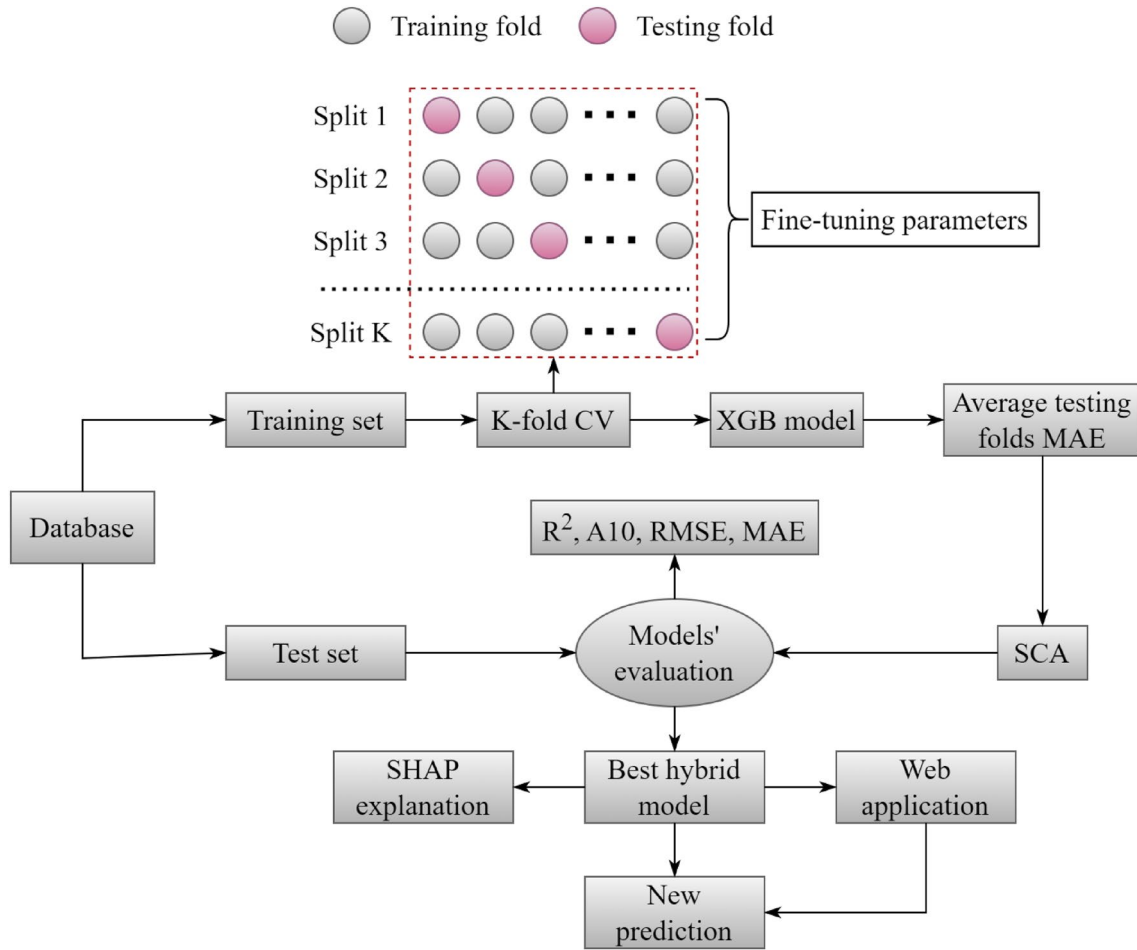
Fig. 4 Flowchart of development of SCA-XGB models

Table 2 Optimal hyperparameters of the XGB model

Hyperparameter	learning_rate	max_depth	n_estimators
Optimized value	0.28763	2	618

Model explanation

To explore the black box of the SCA-XGB model, it is essential to conduct a comprehensive investigation of the effects of various input parameters, such as cement, water, fine aggregate, coarse aggregate, fly ash, superplasticizer, silica fume, nano silica, and temperature, on concrete strength at elevated temperatures.

This study uses the Shapley Additive Explanations (SHAP) method (Lundberg & Lee, 2017) to explain the feature importance of input features and their contribution to concrete strength prediction. The details of the SHAP method can be found somewhere (Lundberg & Lee, 2017; Tran & Kim, 2023). In the SHAP method, the output is calculated based on the baseline value and the Shapley value of the input variables as follows:

$$y_{pred}^{(i)} = y_{base} + \sum_{j=1}^{n} f(x_{ij}) \tag{7}$$

Table 3 Performance of the best SCA-XGB model

Pop size	Ratio	Training set R^2	A10	RMSE	MAE	Test set R^2	A10	RMSE	MAE
100	90–10	0.995	0.925	1.774	1.317	0.982	0.810	3.676	2.706

The unit of RMSE and MAE is MPa

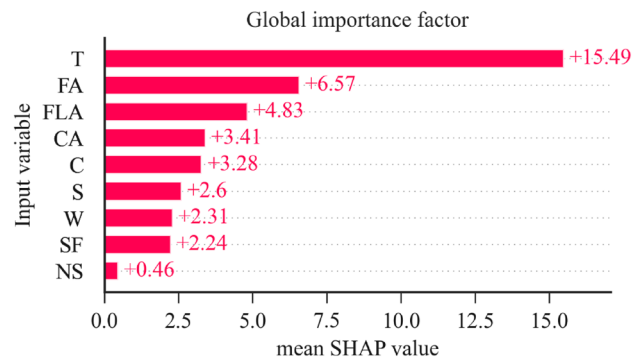**Table 4** Performance of different ML models

Model	Training set				Test set			
	R^2	A10	RMSE	MAE	R^2	A10	RMSE	MAE
SCA-XGB	**0.995**	**0.925**	**1.774**	**1.317**	**0.982**	**0.810**	**3.676**	**2.706**
XGB	1.0	1.0	0.003	0.002	0.965	0.810	4.604	3.595
DT	1.0	1.0	0.0	0.0	0.941	0.619	6.403	4.740
RF	0.985	0.828	3.296	2.109	0.971	0.714	4.425	3.443
AGB	0.941	0.446	7.731	6.410	0.927	0.381	8.679	6.735
GB	0.984	0.839	3.259	2.337	0.967	0.667	4.862	3.613
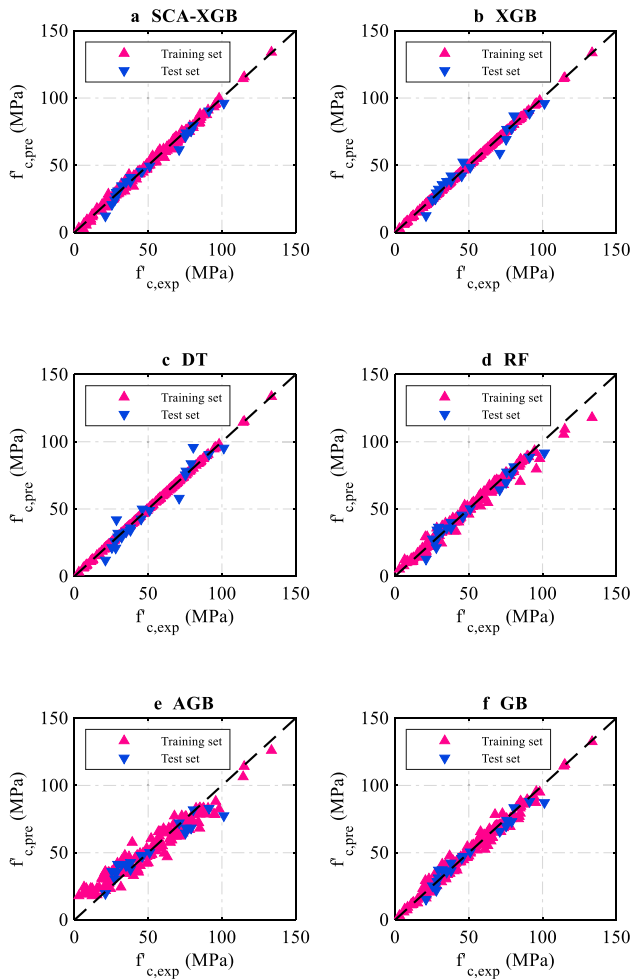
Fig. 5 Scatter plots of different ML models

Fig. 6 Global importance of features

Figure 7 depicts the SHAP summary plot of each input parameter. Each point on the plot indicates a sample data point. The y-axis exhibits the feature names, while the x-axis displays the magnitude of the Shapley value. The feature importances are sorted based on the amplitude of their impact on the prediction in the y-axis. It can be seen that the T has the most significant effect on the concrete strength based on the SCA-XGB model. Notably, a higher value of T and W cause reducing the concrete strength. In contrast, the concrete strength increases if the FA, FLA, CA, C, S, SF, and NS increases.

Figure 8 shows the prediction of specific instances of the database. In this figure, E[f(x)] is the baseline value (average predictive value of the training data), and f(x) is the final prediction value based on the SCA-XGB model. The red bar indicates the positive contribution of the feature. In contrast, the blue bar denotes the negative contribution of the feature. The grey numbers are the normalized values of the input parameters. It can be seen that the prediction (7.941 MPa) is lower than the base value (49.241 MPa). In this specimen, CA (normalized value of 1.988) and W (normalized value of − 1.016) have a positive effect on the concrete strength, which adds 1.82 MPa and 0.38 MPa, respectively, to the prediction from the baseline value (49.241 MPa). However, T (normalized value of 1.536), C (normalized value of − 1.958), FA (normalized value of − 0.69), FLA (normalized value of − 0.4), SF (normalized value of − 0.78), S (normalized
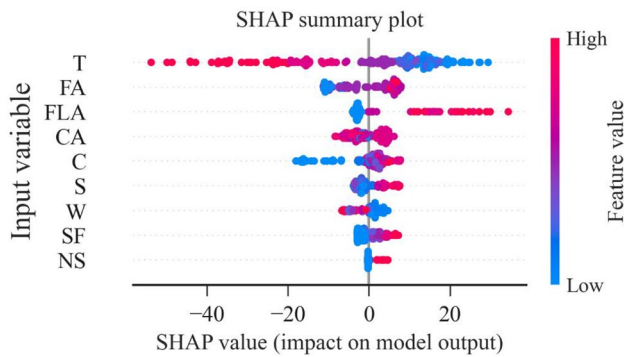
where y_{base} is the baseline value of the ML model; n is the number of input parameters; $f(x_{ij})$ is the Shapley value of the input parameter x_{ij}.

Figure 6 shows the global importance factors of the input variables for the compressive strength prediction. The feature with a higher absolute summation of Shapley values is more important. It can be seen that T has a significant influence on compressive strength prediction, followed by FA, FLA, CA, C, S, W, SF, and NS.
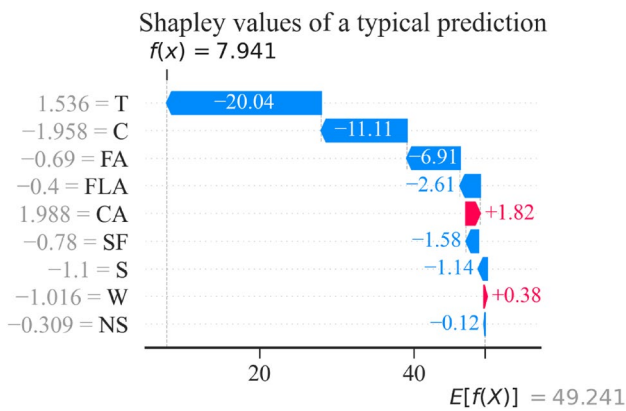
Fig. 7 SHAP summary plot

Fig. 8 Shapley values of a typical prediction

value of – 1.1), and NS (normalized value of – 0.309) have a negative effect on the concrete strength, which decreases the prediction by – 20.04 MPa, – 11.11 MPa, – 6.91 MPa, – 2.61 MPa, – 1.58 MPa, – 1.14 MPa, and – 0.12 MPa, respectively, to the prediction from the baseline value (49.241 MPa).

Web application development

This section aims to create an interactive web application for users unfamiliar with ML algorithms. The web application is developed based on a Streamlit platform to facilitate the prediction of concrete strength at elevated temperatures. Users can directly measure concrete strength using nine input parameters. Accordingly, using the web application can save

time and effort in estimating the concrete strength at elevated temperatures in the pre-design process. The web application interface is shown in the Appendix. The accessed link of the web application can be found here: https://tvl-concretestrength-hightemperature.streamlit.app/.

Conclusions

This study develops a novel hybrid ML model, called SCA-XGB, that integrates a sine cosine algorithm and an extreme gradient boosting, to enhance the prediction of concrete compressive strength at elevated temperatures. The SHAP method explores the effect of different input features on the concrete compressive strength. An effective web tool is developed for practical applications. Some conclusions are stated as follows:

(1) The SCA-XGB model achieves the lowest values of the errors (RMSE of 3.676 MPa and MAE of 2.706 MPa) and the highest correlation (R^2 of 0.982 and A10 of 0.810) in the test phase. It demonstrates remarkable performance, achieving high accuracy and robustness compared to other ML models (i.e., XGB, DT, RF, AGB, and GB). It is indicated that the SCA proves to be effective in improving the XGB's predictive capability.

(2) Compared with the XGB, DT, RF, AGB, and GB models, R^2 and A10 increased by (1.762%, 4.357%, 1.133%, 5.933%, and 1.551%) and (0.0%, 30.856%, 13.445%, 112.598%, and 21.439%), RMSE and MAE decreased by (20.156%, 42.589%, 16.927%, 57.645%, and 24.393%) and (24.729%, 42.911%, 21.406%, 59.822%, and 25.104%), respectively, in the SCA-XGB model in the test phase.

(3) The SHAP method shows that T has a significant influence on compressive strength prediction, followed by FA, FLA, CA, C, S, W, SF, and NS.

(4) The web application is considered an efficient tool for accurate concrete strength prediction at elevated temperatures, which can be successfully adopted for concrete strength prediction without spending time and cost on experimental work in the laboratory.

It is noted that ML algorithms depend significantly on the amounts and quality of training data. It should be possible to improve ML models' accuracy using updated data with diverse input parameters in future work.

Appendix

Web application interface

Development of an explainable predictive hybrid SCA-XGB model for compressive strength of concrete at elevated temperatures
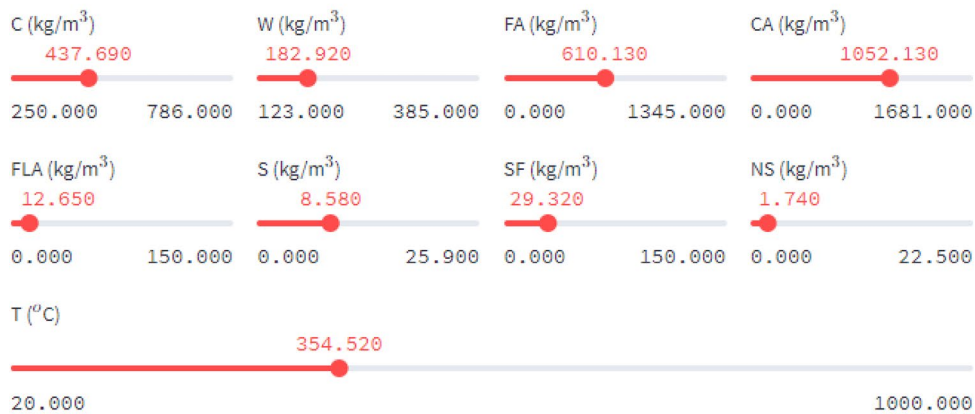
1. Flowchart
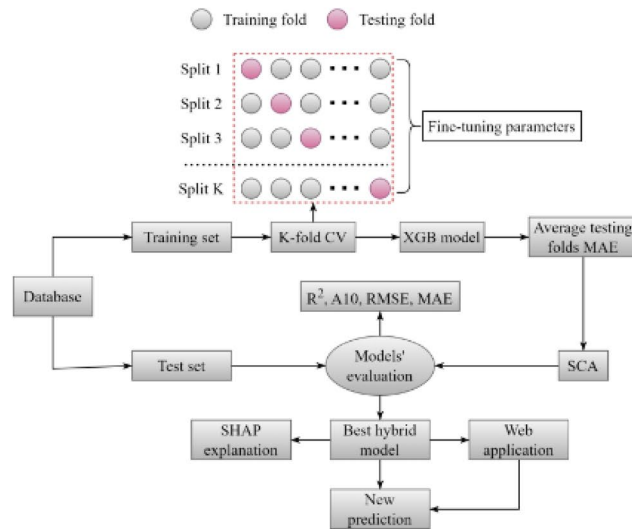
2. Database

☐ 2.1. Preview database

☐ 2.2. Show summary of database

☐ 2.3. Data distribution

3. Predicting the concrete strength

C (kg/m^3)		W (kg/m^3)		FA (kg/m^3)		CA (kg/m^3)	
437.690		182.920		610.130		1052.130	
250.000	786.000	123.000	385.000	0.000	1345.000	0.000	1681.000

FLA (kg/m^3)		S (kg/m^3)		SF (kg/m^3)		NS (kg/m^3)	
12.650		8.580		29.320		1.740	
0.000	150.000	0.000	25.900	0.000	150.000	0.000	22.500

T (^{o}C)	
354.520	
20.000	1000.000

Concrete strength is 46.401 (MPa)

Declarations

References

Abbas, H., Al-Salloum, Y. A., Elsanadedy, H. M., & Almusallam, T. H. (2019). ANN models for prediction of residual strength of HSC after exposure to elevated temperature. *Fire Safety Journal, 106*, 13–28. https://doi.org/10.1016/j.firesaf.2019.03.011

Ahmad, A., Ostrowski, K. A., Maślak, M., Farooq, F., Mehmood, I., & Nafees, A. (2021). Comparative study of supervised machine learning algorithms for predicting the compressive strength of concrete at high temperature. *Materials, 14*(15), 4222. https://doi.org/10.3390/ma14154222

An, J., Mikhaylov, A., & Richter, U. H. (2020). Trade war effects: evidence from sectors of energy and resources in Africa. *Heliyon, 6*(12), e05693. https://doi.org/10.1016/j.heliyon.2020.e05693

Chan, Y. N., Luo, X., & Sun, W. (2000). Compressive strength and pore structure of high-performance concrete after exposure to high temperature up to 800 °C. *Cement and Concrete Research, 30*(2), 247–251. https://doi.org/10.1016/S0008-8846(99)00240-9

Chen, T., & Guestrin, C. (2016). XGBoost: a scalable tree boosting system. In *Proceedings of the ACM SIGKDD International Conference on Knowledge Discovery and Data Mining* (Vol. 13–17-Augu, pp. 785–794). New York, NY, USA: ACM. https://doi.org/10.1145/2939672.2939785

Chica, L., & Alzate, A. (2019). Cellular concrete review: New trends for application in construction. *Construction and Building Materials, 200*, 637–647. https://doi.org/10.1016/j.conbuildmat.2018.12.136

Dinesh, A., Anitha Selvasofia, S. D., Datcheen, K. S., & Rakhesh Varshan, D. (2023). Machine learning for strength evaluation of concrete structures – critical review. *Materials Today: Proceedings.* https://doi.org/10.1016/j.matpr.2023.04.090

Dong, B., Wang, F., Abadikhah, H., Hao, L., Xu, X., Khan, S. A., & Agathopoulos, S. (2019). Simple fabrication of concrete with remarkable self-cleaning ability, robust superhydrophobicity, tailored porosity, and highly thermal and sound insulation. *ACS Applied Materials & Interfaces, 11*(45), 42801–42807. https://doi.org/10.1021/acsami.9b14929

Gupta, S., Kua, H. W., & Pang, S. D. (2020). Effect of biochar on mechanical and permeability properties of concrete exposed to elevated temperature. *Construction and Building Materials, 234*, 117338. https://doi.org/10.1016/j.conbuildmat.2019.117338

Huber, F., Yushchenko, A., Stratmann, B., & Steinhage, V. (2022). Extreme gradient boosting for yield estimation compared with deep learning approaches. *Computers and Electronics in Agriculture, 202*, 107346. https://doi.org/10.1016/j.compag.2022.107346

Husem, M. (2006). The effects of high temperature on compressive and flexural strengths of ordinary and high-performance concrete. *Fire Safety Journal, 41*(2), 155–163. https://doi.org/10.1016/j.firesaf.2005.12.002

Kaloop, M. R., Kumar, D., Samui, P., Hu, J. W., & Kim, D. (2020). Compressive strength prediction of high-performance concrete using gradient tree boosting machine. *Construction and Building Materials.* https://doi.org/10.1016/j.conbuildmat.2020.120198

Karahan, O. (2017). Transport properties of high volume fly ash or slag concrete exposed to high temperature. *Construction and Building Materials, 152*, 898–906. https://doi.org/10.1016/j.conbuildmat.2017.07.051

Kaveh, A. (2021). *Advances in metaheuristic algorithms for optimal design of structures.* Springer. https://doi.org/10.1007/978-3-030-59392-6

Kaveh, A., Dadras Eslamlou, A., & Mahdipour Moghani, R. (2021). Shear strength prediction of FRP-reinforced concrete beams using an extreme gradient boosting framework. *Periodica Polytechnica Civil Engineering.* https://doi.org/10.3311/PPci.18901

Kaveh, A., & Iranmanesh, A. (1998). Comparative study of backpropagation and improved counterpropagation neural nets in structural analysis and optimization. *International Journal of Space Structures, 13*(4), 177–185. https://doi.org/10.1177/026635119801300401

Kim, J.-K., Han, S. H., & Song, Y. C. (2002). Effect of temperature and aging on the mechanical properties of concrete. *Cement and Concrete Research, 32*(7), 1087–1094. https://doi.org/10.1016/S0008-8846(02)00744-5

Li, L., Khan, M., Bai, C., & Shi, K. (2021). Uniaxial tensile behavior, flexural properties, empirical calculation and microstructure of multi-scale fiber reinforced cement-based material at elevated temperature. *Materials, 14*(8), 1827. https://doi.org/10.3390/ma14081827

Lundberg, S. M., & Lee, S. I. (2017). A unified approach to interpreting model predictions. *Advances in Neural Information Processing Systems.* https://doi.org/10.48550/arXiv.1705.07874

Ma, Q., Guo, R., Zhao, Z., Lin, Z., & He, K. (2015). Mechanical properties of concrete at high temperature—a review. *Construction and Building Materials, 93*, 371–383. https://doi.org/10.1016/j.conbuildmat.2015.05.131

Mai, S. H., Nguyen, D. H., Tran, V.-L., & Thai, D.-K. (2023). Development of hybrid machine learning models for predicting permanent transverse displacement of circular hollow section steel members under impact loads. *Buildings, 13*(6), 1384. https://doi.org/10.3390/buildings13061384

Masaki, K., & Maki, I. (2002). Effect of prolonged heating at elevated temperatures on the phase composition and textures of Portland cement clinker. *Cement and Concrete Research, 32*(6), 931–934. https://doi.org/10.1016/S0008-8846(02)00726-3

Memon, S. A., Shah, S. F. A., Khushnood, R. A., & Baloch, W. L. (2019). Durability of sustainable concrete subjected to elevated temperature – a review. *Construction and Building Materials, 199*, 435–455. https://doi.org/10.1016/j.conbuildmat.2018.12.040

Mirjalili, S. (2016). SCA: a sine cosine algorithm for solving optimization problems. *Knowledge-Based Systems, 96*, 120–133. https://doi.org/10.1016/j.knosys.2015.12.022

Mirjalili, S., & Gandomi, A. H. (2023). *Comprehensive metaheuristics algorithms and applications.* Academic Press. https://doi.org/10.1016/C2021-0-01466-8

Mukherjee, A., & Nag Biswas, S. (1997). Artificial neural networks in prediction of mechanical behavior of concrete at high temperature. *Nuclear Engineering and Design, 178*(1), 1–11. https://doi.org/10.1016/S0029-5493(97)00152-0

Naderpour, H., Rafiean, A. H., & Fakharian, P. (2018). Compressive strength prediction of environmentally friendly concrete using artificial neural networks. *Journal of Building Engineering, 16*(January), 213–219. https://doi.org/10.1016/j.jobe.2018.01.007

Nguyen, K. T. Q., Navaratnam, S., Mendis, P., Zhang, K., Barnett, J., & Wang, H. (2020). Fire safety of composites in prefabricated buildings: From fibre reinforced polymer to textile reinforced concrete. *Composites Part B Engineering, 187*, 107815. https://doi.org/10.1016/j.compositesb.2020.107815

Nguyen, N.-H., Abellán-García, J., Lee, S., Garcia-Castano, E., & Vo, T. P. (2022a). Efficient estimating compressive strength of ultra-high performance concrete using XGBoost model. *Journal of Building Engineering, 52*, 104302. https://doi.org/10.1016/j.jobe.2022.104302

Nguyen, V. Q., Tran, V. L., Nguyen, D. D., Sadiq, S., & Park, D. (2022b). Novel hybrid MFO-XGBoost model for predicting the racking ratio of the rectangular tunnels subjected to seismic loading. *Transportation Geotechnics, 37*, 100878. https://doi.org/10.1016/j.trgeo.2022.100878

Reiter, L., Wangler, T., Anton, A., & Flatt, R. J. (2020). Setting on demand for digital concrete – principles, measurements, chemistry, validation. *Cement and Concrete Research, 132*, 106047. https://doi.org/10.1016/j.cemconres.2020.106047

Roy, T., & Matsagar, V. (2021). Mechanics of damage in reinforced concrete member under post-blast fire scenario. *Structures, 31*, 740–760. https://doi.org/10.1016/j.istruc.2021.02.005

Salehi, H., & Burgueño, R. (2018). Emerging artificial intelligence methods in structural engineering. *Engineering Structures, 171*(May), 170–189. https://doi.org/10.1016/j.engstruct.2018.05.084

Tanyildizi, H., & Coskun, A. (2008). Performance of lightweight concrete with silica fume after high temperature. *Construction and Building Materials, 22*(10), 2124–2129. https://doi.org/10.1016/j.conbuildmat.2007.07.017

Thai, H. T. (2022). Machine learning for structural engineering: a state-of-the-art review. *Structures, 38*, 448–491. https://doi.org/10.1016/j.istruc.2022.02.003

Tran, V. L., Ahmed, M., & Gohari, S. (2023). Prediction of the ultimate axial load of circular concrete-filled stainless steel tubular columns using machine learning approaches. *Structural Concrete.* https://doi.org/10.1002/suco.202200877

Tran, V. L., & Kim, J. K. (2023). Ensemble machine learning-based models for estimating the transfer length of strands in PSC beams. *Expert Systems with Applications, 221*, 119768. https://doi.org/10.1016/j.eswa.2023.119768

Van Nguyen, D., Kim, D., & Choo, Y. (2022c). Optimized extreme gradient boosting machine learning for estimating diaphragm wall deflection of 3D deep braced excavation in sand. *Structures, 45*, 1936–1948. https://doi.org/10.1016/j.istruc.2022.10.027